https://doi.org/10.5194/egusphere-2025-6006
Preprint. Discussion started: 18 December 2025


# Year-Round Characterization of Upwelling Along the Uruguayan Coast Using a High-Resolution Regional Ocean Model

Camila de Mello[1], Marcelo Barreiro[1] and Madeleine Renom[1]

[1]Department of Atmospheric and Oceanic Sciences, Institute of Physics, Universidad de la República, Iguá 4225, Montevideo 11400, Uruguay

*Correspondence to*: Camila de Mello (camila.demello@fcien.edu.uy)

**Abstract.** Upwelling along the Uruguayan coast has largely been interpreted as a summertime process, primarily based on surface temperature signals. Here, we investigate coastal upwelling year-round using a high-resolution regional ocean model (Coastal and Regional Ocean Community, CROCO), with the aim of reassessing how upwelling manifests across seasons under contrasting thermohaline conditions. The seasonal covariability between daily winds and sea surface salinity anomalies was analyzed through a Maximum Covariance Analysis, revealing upwelling signatures during spring, autumn, and summer, marked by positive sea surface salinity anomalies (SSSa) along the Uruguayan coast. Summer upwelling events were characterized by positive SSSa and negative sea surface temperature anomalies (SSTa), indicating that both are reliable upwelling proxies during this season. In contrast, during spring and autumn, SSSa resulted in a better proxy. In this regard, upwellings were clearly marked by increments in SSSa, but the SSTa pattern in the coast was variable due to differences in thermal vertical profiles. Based on the thermal properties of the upwelled waters, three upwelling regimes can be identified: cold-water upwellings associated with warm-season stratified conditions, transitional upwelling events occurring under weak or absent thermal stratification, and warm-water upwellings linked to cold-season conditions, characterized by inverse thermal stratification. Overall, our results highlight that upwelling events along the Uruguayan coast cannot be described by a single thermal signature, but rather by seasonally dependent thermohaline regimes.

## 1. Introduction

The Uruguayan coastal and estuarine region is part of a highly dynamic system characterized by strong spatial and temporal variability driven by atmospheric forcing and variable Río de la Plata freshwater discharge (Guerrero and Piola, 1997; Nagy et al., 2002; Piola et al., 2005; Acha et al., 2008; Ortega and Martínez, 2007; Martínez and Ortega, 2015). Within this system, wind-driven upwelling is a relevant process with the potential to modulate coastal circulation and surface hydrographic properties (Simionato et al., 2010; Meccia et al., 2013; Trinchin et al., 2019; de Mello et al., 2022a).

https://doi.org/10.5194/egusphere-2025-6006
Preprint. Discussion started: 18 December 2025


Most of the current understanding of upwelling along the Uruguayan coast has been derived from satellite observations and numerical modeling studies, motivated in part by the limited availability of continuous in situ data with adequate spatial coverage. These studies have documented the spatial structure, temporal variability, and three-dimensional characteristics of wind-induced upwelling during summer, when alongshore winds are more frequent and thermal stratification tends to enhance the surface expression of upwelling (Simionato et al., 2010; Meccia et al., 2013; Trinchin et al., 2019; de Mello et al., 2022a,b; de Mello et al., 2023).

Consequently, previous studies have focused exclusively on summertime upwelling. Although easterly winds are more frequent and persistent during summer, upwelling-favorable winds can occur throughout the year (Simionato et al., 2005). While the underlying mechanism is expected to be similar, the properties of the upwelled waters and their surface expression are likely to differ across seasons due to changes in surface heat fluxes and vertical thermal structure.

During summer, atmospheric heat fluxes warm surface waters, enhancing vertical temperature stratification. Outside of summer, surface heat fluxes may result in weak or even inverse temperature stratification near the coast during transitional months, with warmer but saltier waters near the bottom. Consequently, upwelled water may exhibit different SST characteristics depending on the timing of the event, complicating their identification through the SST distribution.

Beyond its physical expression, coastal upwelling can have significant ecological and socioeconomic impacts. Upwelling-related frontal regions may enhance nutrient retention in bays, promote phytoplankton blooms, and favor the accumulation of early life stages, with potential consequences for higher trophic levels (Pitcher et al., 2010; Largier, 2020; de Mello et al., 2022b). In addition, circulation patterns associated with upwelling can influence the offshore transport of suspended material and organisms, as documented for summertime events along the Uruguayan coast (de Mello et al., 2023). However, the occurrence of upwelling outside the summer season, as well as its associated impacts, remains largely unexplored.

In this context, Sea Surface Salinity (SSS) distribution could serve as an alternative proxy to SST for identifying upwelling along the Uruguayan coast throughout the year, as the water column is expected to remain on average vertically stratified with saltier water closer to the bottom, as this is a salt wedge estuary (Guerrero et al., 1997). Therefore, during upwelling the surface water would likely show positive SSS anomalies regardless of the time of year. In this regard, increased surface salinity in the Uruguayan coast (particularly between Montevideo and Punta del Este) under

https://doi.org/10.5194/egusphere-2025-6006
Preprint. Discussion started: 18 December 2025


upwelling-favorable wind conditions has been reported in numerical simulations (Meccia et al., 2008; de Mello et al., 2022).

However, despite the availability of localized in situ observations of temperature and salinity vertical structure from specific oceanographic campaigns (e.g., Pimenta et al., 2008; Burone et al., 2013; BaRDO Database), there is no comprehensive characterization of the mean water column properties along the coast, nor a systematic description of year-round upwelling based on salinity in the region, highlighting the importance of numerical simulations for understanding upwelling processes and their characteristics.

To enhance our understanding of upwelling along the Uruguayan coast, the CROCO model was configured with an interannual setup (similar to that used by de Mello et al., 2023, but covering a longer period) to identify and characterize upwelling events occurring throughout the year. We employed a Maximum Covariance Analysis between simulated SSS and zonal wind anomalies. Given the expected changes in the vertical thermal profiles near the coast throughout the year, SST might not be a reliable proxy for identifying wind-induced upwelling events outside summer. Therefore, we propose using SSS anomalies in conjunction with surface winds to detect upwelling events across seasons.

This article is organized as follows: **Section 2** briefly describes the model setup and validates its ability to represent the mean and interannual variability of surface coastal fields throughout the year by comparing model results with reanalyses, observational data, and published studies. It also presents the mean simulated vertical profiles of salinity and temperature near the coastal region. In **Section 3**, we perform a Maximum Covariance Analysis (MCA) between zonal surface winds and simulated SSS anomalies to identify the dates when the most intense upwelling events occur throughout the year, and which are studied in subsequent sections. **Section 4** examines the mean distribution of SSTa and SSSa during the upwelling dates and compares the simulated SSTa pattern with observed data. In **Section 5**, we analyze specific upwelling events occurring during spring and autumn and their vertical profiles. Finally, **Section 6** summarizes the conclusions and provides final remarks.

## 2. Numerical Ocean Model

### 2.1 Model Setup

The model used in this study is the Coastal and Regional Ocean Community Model CROCO, https://www.croco-ocean.org/). It is designed for simulating high-resolution offshore and nearshore

https://doi.org/10.5194/egusphere-2025-6006
Preprint. Discussion started: 18 December 2025


dynamics in regional domain configurations (Shchepetkin and McWilliams, 2005; Debreu et al., 2012). CROCO is a split-explicit free surface, and σ terrain-following vertical coordinate oceanic model configured with a horizontal resolution of 1/36° (about 2.5 km in the region of interest) and 40 σ vertical layers. The model bathymetry is derived from the 1 min Gridded Global Relief Data (ETOPO1) topography (Amante and Eakins, 2009), interpolated to the model grid, and modified to reduce horizontal pressure gradient errors. The simulated domain considers the area defined by 31° S - 36° S and 50° W - 59° W, which includes the Uruguayan coast (Figure 1). It has open boundaries in the eastern, western and southern boundaries. All lateral boundary conditions were obtained from the GLORYS reanalysis (Lellouche et al., 2018) at 1/12° of horizontal resolution for the period 1993–2020.

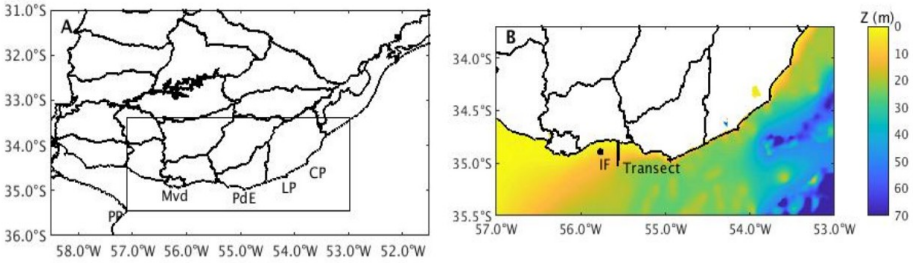


Figure 1: (A) Study area where the CROCO model was set up. The inner rectangle corresponds to the area where the model results were analyzed and considered for identifying upwellings. Mvd: Montevideo, PdE: Punta del Este, LP: La Paloma, CP: Cabo Polonio (B) ETOPO1 bathymetry (color scale is in meters). IF marks the Isla de Flores location, where surface temperature and salinity data were considered to compare model with observations, CL marks the coastal location where the vertical average temperature and salinity simulated profiles were obtained for each season; and TR marks the section where the simulated upwelling vertical structure was analyzed.

Interannual daily Río de la Plata freshwater discharge was provided by the Instituto Nacional del Agua in Argentina (Borús, 2022), and introduced in the model divided into 2 source points at the Rio de la Plata's head. Daily wind stress from NCEP-DOE Reanalysis 2, for the period 1993–2020 (Kanamitsu et al., 2002), as well as monthly mean heat and freshwater (precipitation minus evaporation) fluxes derived from the Comprehensive Ocean Atmosphere Data Set (COADS, da Silva et al., 1994) were used to force the model. Further description of the model configuration can be found in de Mello et al. (2022a and 2023). As de Mello et al. (2023) the model includes tidal forcing. Mean and instantaneous fields for the period 2005 - 2020 were saved every day.

https://doi.org/10.5194/egusphere-2025-6006
Preprint. Discussion started: 18 December 2025


### 2.2 Simulated fields and Validation

The simulated variables were compared with reanalysis, observational and published data. The simulated mean and daily variability of SST, SSS and surface currents were compared with the GLORYS reanalysis, which was used as lateral boundary conditions. Also daily SSS and SST variability were compared to in situ data at the coastal location Isla de Flores (IF) marked in Figure 1B; 55.9 °W - 34.9 °S (Trinchin et al., 2020; Brum, 2024). Overall a satisfactory representation of the regional coastal surface currents, salinity and temperature distribution was reproduced by the model. The simulation outputs were similar to those obtained by de Mello et al. (2022a and 2023), which used a similar configuration but for a shorter period. A detailed description and validation of the model outputs (explicitly for the summer period) can be found in de Mello et al. (2022a).

Close to the coast, the circulation is dominated by currents that run parallel to the coast, which are stronger in CROCO compared to GLORYS (possibly due to the higher resolution). The simulated mean sea surface temperature is concordant with the literature (Guerrero et al.,1997; Möller et al., 2008; Simionato et al., 2010; Guerrero et al., 2010; Rabellino, 2016). Nevertheless, compared to GLORYS, the model has a cold bias located mainly in the oceanic and offshore area, as observed in the Mello et al., 2022 for the summer period. A marked east-west Sea Surface Salinity (SSS) gradient along the estuary axis is observed in the surface and reproduced by the model (Piola et al., 2000, Möller et al., 2008; Piola et al., 2008; Guerrero et al., 1997; Guerrero et al., 2010). Surface comparisons of the mean results of Sea Surface Temperature (SST) and Sea Surface Salinity (SSS) between CROCO and the GLORYS reanalysis are included in Figure 2 (A-D).

At the coastal location of Isla de Flores (55.9°W, 34.9°S), the model simulates the daily mean and variability of both SST and SSS. The simulated climatological SST and SSS closely match observed climatological values (Brum, 2024; Trinchin et al., 2021; Trinchin et al., 2024). The highest simulated climatological temperature occurs in February (23.7°C), while July is the month with the lowest average simulated temperature (11.3°C), consistent with in situ observations. Similarly, the simulated salinity values fall within the range of observed values for Isla de Flores, with the highest monthly average salinity occurring in December (22.0) and the lowest in July (11.4), consistent with observations. However, the minimum average simulated salinity is slightly lower than the climatological measurements. It's important to note that the in situ data we compared against is from a five-year series (2018 to 2023), during which the region experienced a drought between 2020 and 2022, leading to extremely low freshwater discharges from the Río de la Plata

https://doi.org/10.5194/egusphere-2025-6006
Preprint. Discussion started: 18 December 2025


and consequently affecting coastal salinity. Therefore, some differences between the simulated and observed climatological values were expected.

A comparison between CROCO and GLORYS reanalysis data at the Isla de Flores location shows a
155 significant daily correlation for SST and SSS during the period 2005–2020, with correlation coefficients of 0.97 and 0.62, respectively. A comparison between CROCO-simulated and in situ measured SST and SSS at Isla de Flores for the period May 2019 to April 2020 is presented in Figure 2 E-F. Both correlations are significant, with r=0.96 for SST and r=0.41 for SSS.

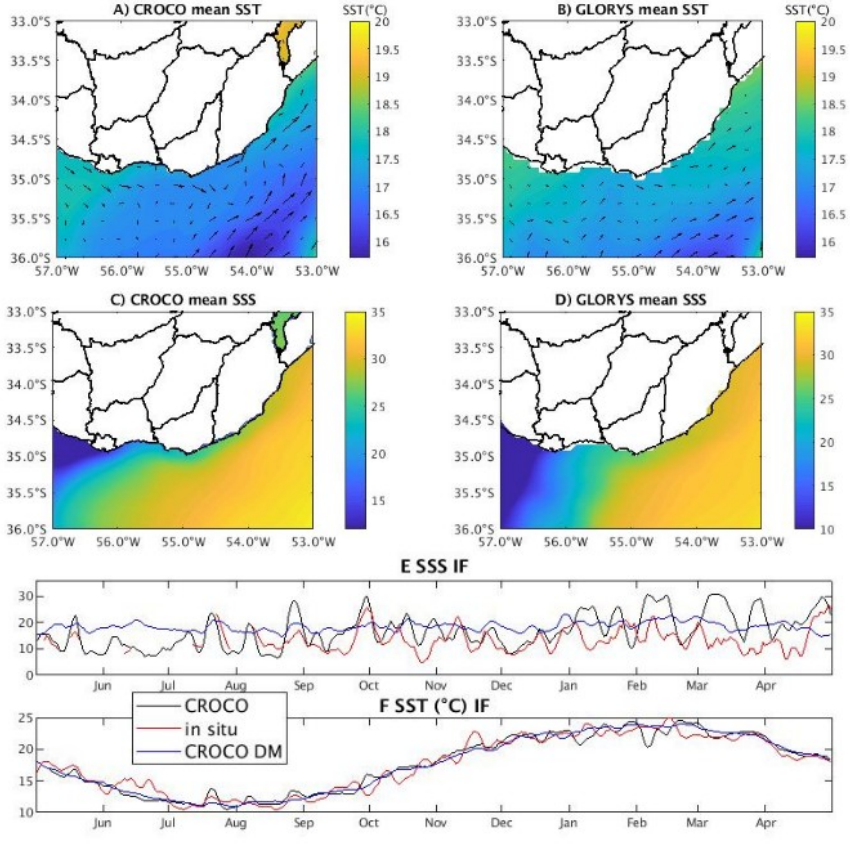


160 Figure 2: Mean SST (°C) and velocity vectors, and mean SSS simulated by CROCO (A and C) and by GLORYS reanalysis (B and D). Evolution of daily SST (E) and SSS (F) for the period May 2019 – April 2020 simulated by CROCO (black line), and measured in situ (red line) at Isla de Flores Location. The CROCO daily mean (DM) is shown in blue line for both plots.

https://doi.org/10.5194/egusphere-2025-6006
Preprint. Discussion started: 18 December 2025


Vertical simulated profiles align well with the GLORYS Reanalysis and are consistent with the patterns observed in climatological atlases based on in situ measurements showing warmer and fresher waters at surface along the Uruguayan coast during the warm season, and colder (yet still fresher) waters at surface along the coast during the cold season (Guerrero et al., 2010; Baldoni et al., 2015). In the Coastal Location (CL, Figure 1B) climatological simulated salinity profiles consistently show an average stratified pattern throughout the year, with fresher waters near the surface. Temperature profiles, however, reveal marked seasonal differences. During summer, the model indicates vertical stratification, consistent with heat influx warming the surface waters. As autumn progresses, surface waters begin losing heat to the atmosphere, reducing both temperature and stratification, leading to a generally weak inverse vertical pattern, and a pronounced inverse stratification in winter. Finally, as spring advances, surface waters warm again, reducing the inverse thermal stratification and resulting in an almost mean unstratified pattern for the spring trimester (Figure 3).

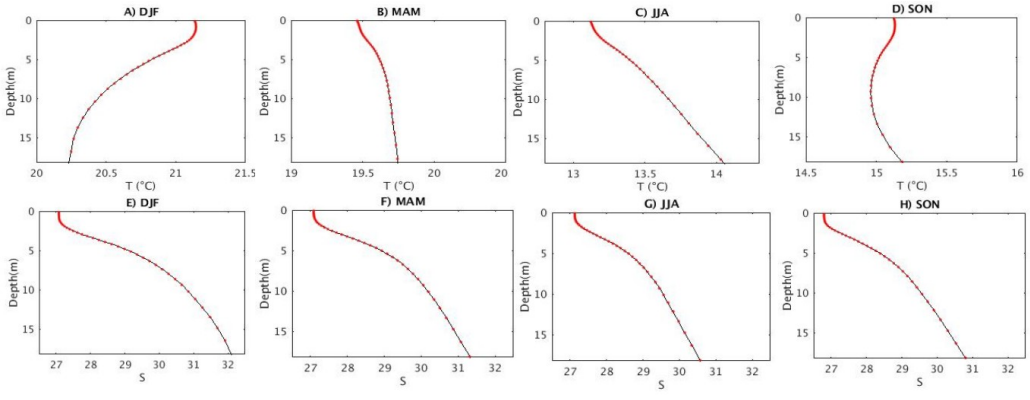


Figure 3: Simulated seasonal average vertical profiles of temperature (A-D) and salinity (E-H) at a coastal location (35.1°S, 55°W). Different scales were used for temperature profiles.

The limited availability of in situ data prevents the development of a reliable climatology for direct comparison with our simulations, emphasizing the importance of numerical modeling for understanding coastal dynamics. Despite the lack of continuous observational data to construct climatological profiles, a consistent pattern with the simulations was observed during an Argentine research campaign conducted aboard the *Dr. Eduardo Holmberg* vessel in June 2006 (BaRDO, INIDEP). During this campaign, several samples were collected in the Uruguayan coastal zone. These allowed for a comparison between the average vertical profiles from stations located in the estuarine and oceanic regions; and the average profiles simulated by CROCO for the same locations

https://doi.org/10.5194/egusphere-2025-6006
Preprint. Discussion started: 18 December 2025


and period. The observed and simulated profiles were found to be consistent with the winter climatological simulated profile, showing warmer and saltier waters at depth for both regions (Figure 4).

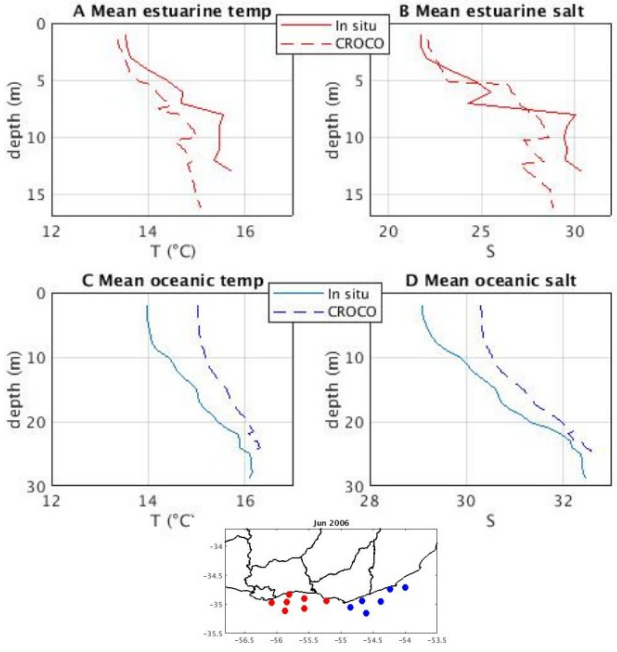


Figure 4: Mean vertical profiles of temperature and salinity simulated by the model (dashed lines) and observed (solid lines) during June 2006. Profiles correspond to stations located in the estuarine region (A and B, red dots in the inset map) and in the oceanic region (B and C, blue dots in the inset map).

## 3. Identification of intense upwelling

To detect intense upwelling occurring directly related to the wind, a Maximum Covariance Analysis (MCA, Wallace et al., 1992) between the daily mean simulated SSS anomalies (SSSa) and the zonal component of daily surface wind anomalies for the period 2005-2020 was applied for each season: December-January-February (DJF), March-April-May (MAM), June-July-August (JJA) and September-October-November (SON). This statistical technique finds patterns in two space-time data sets that explain the maximum fraction of the covariance between them and provides insight into the physical processes that lead to the spatial and temporal variations exhibited in the fields being analyzed. Daily SSSa were computed as the difference between the simulated value and the

https://doi.org/10.5194/egusphere-2025-6006
Preprint. Discussion started: 18 December 2025


simulated daily climatology. The daily climatology was smoothed considering a 5-day moving average. Anomalies were also detrended previous to the analysis.

For spring (SON), summer (DJF) and autumn (MAM), the leading mode of the MCA applied to the model output represents coastal upwelling, with maximum coastal amplitude from Montevideo to La Paloma (for DJF and MAM) and from Montevideo to Punta del Este for SON; and explained 87%, 79% and 77% of the variance, respectively. With this approximation, we did not find a clear upwelling pattern during winter (Figure 5, G and H).

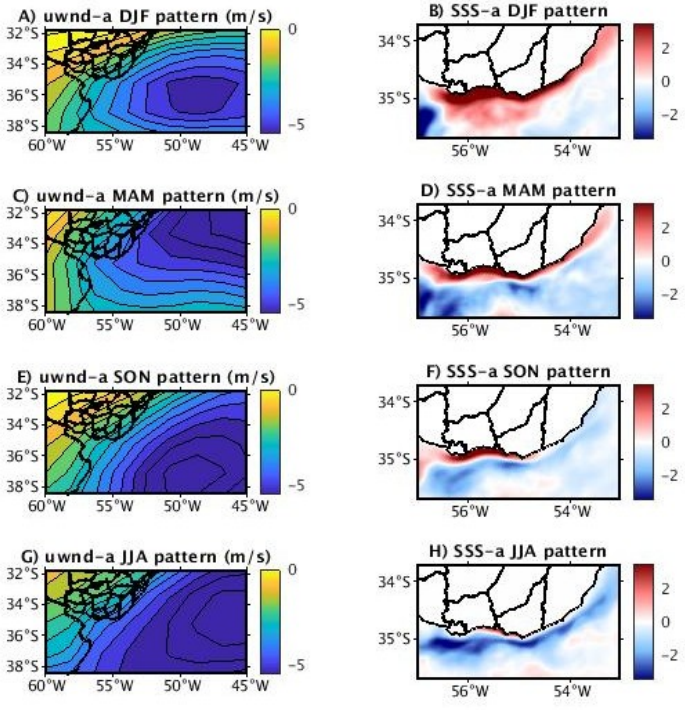


Figure 5: SVD leading mode for each season. A,C,E and G represent the u-wind anomalies pattern while B, D, F and H represent the Sea Surface Salinity anomalies pattern for each analyzed season (summer, autumn, spring and winter, respectively).

## 4. Average distribution of SSTa and SSSa during upwelling dates

To identify intense upwelling dates during summer, autumn, and spring, we employed a statistical analysis method similar to that used by de Mello et al. (2022a, 2023) applied to simulated SSSa instead of SSTa. Intense upwelling dates were considered as those when the time series of simulated

https://doi.org/10.5194/egusphere-2025-6006
Preprint. Discussion started: 18 December 2025


SSSa (Figure 5 B, D, and F) exceeded +1.5 standard deviations for each analyzed season. During summer, events lasting up to 10 days were observed, while in spring and autumn, they were shorter (Figure 6). This finding is consistent with the stronger influence and persistence of easterly winds driving upwelling during summer (Simionato et al. 2005). It is important to note that a rather restrictive definition was used when selecting intense upwelling events, which may have excluded the initial dates of some events where anomalies were smaller. As a result, the actual duration of many events might be slightly longer than identified.

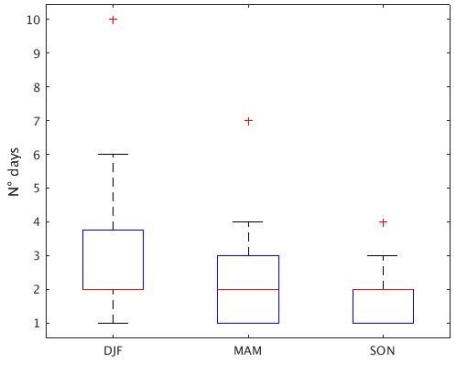


Figure 6: Distribution of intense upwelling events duration for each season

Composites of simulated SSSa and SSTa for the identified upwelling dates (Figure 7 A-F), along with composites of observed SSTa (obtained from the Group of High Resolution Sea Surface Temperature, MUR-GHRSST; Chin et al., 2017) during the same dates were constructed to assess the model's accuracy in representing real patterns during simulated upwelling events (Figure 7 G-I).

The SSSa distribution during upwelling dates revealed a pattern similar to the first SVD mode for each season, with saltier waters near the coast, consistent with deeper saltier waters surfacing during upwelling. On average, during summer upwelling dates, anomalously saltier waters extended farther offshore compared to spring and autumn dates, reaching up to 60 km offshore during summer, 35 km during autumn, and 12 km during spring off the coast of Montevideo (Figure 7 A-C).

https://doi.org/10.5194/egusphere-2025-6006
Preprint. Discussion started: 18 December 2025


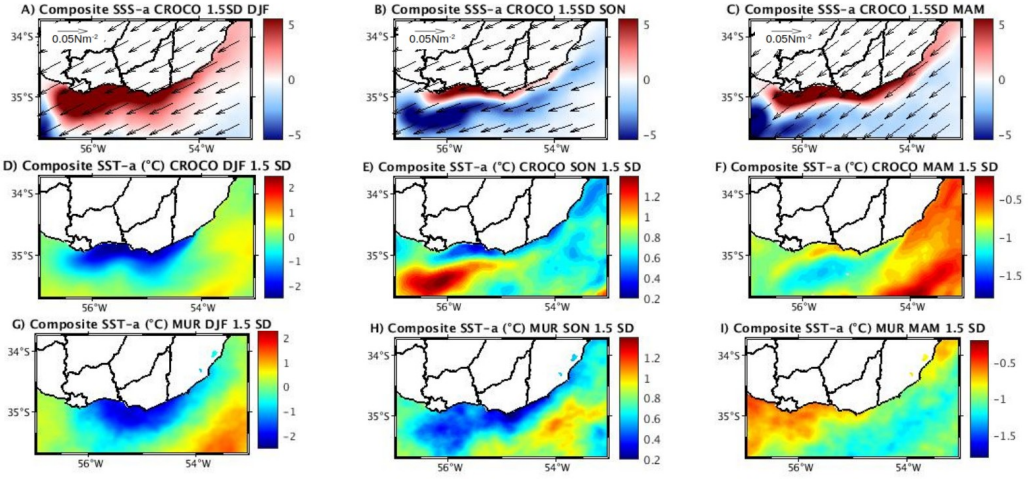


Figure 7: Composites of simulated SSSa (A, B and C), SSTa (D, E and F) and observed SSTa (G, H, I) during upwelling upwelling dates. Note in SSTa different color scales are shown between seasons in order to mark the spatial patterns. Composites of wind stress anomalies (Nm− 2) are shown.

The simulated and observed SSTa composites patterns were consistent (Figure 7 D-I), though some differences were expected due to model biases, as discussed in the previous section and in de Mello et al. (2022a, b and 2023). Seasonal variations in SST anomaly patterns were evident. During summer, an inverse relationship between SSTa and SSSa was observed, with colder, saltier water surfacing during upwelling events (Figure 7 A-D), a pattern also identified by de Mello et al. (2022a and 2023). As shown in Figure 3, summer typically features both thermal and salinity vertical stratification, indicating that upwelled water would be colder and saltier, making upwelling events distinguishable through both salinity and temperature surface anomalies.

Both intermediate seasons, autumn and spring, exhibited different average SSTa distribution patterns during upwelling events. In autumn, SSTa were negative along the coast, with less intense anomalies nearshore compared to offshore. In contrast, during spring, SSTa were positive along the coast, with warm anomalies nearshore but less intense than those offshore (Figure 7 E and F). It is noteworthy that on average during both seasons, the coastal region shows vertical salinity stratification but lacks significant thermal stratification (Figure 3). As autumn progresses, surface temperatures decrease, leading to reduced thermal stratification until winter, when an inverse stratification pattern emerges. Conversely in spring, surface waters warm, gradually increasing thermal stratification. Consequently, the timing of upwelling events in these seasons leads to

https://doi.org/10.5194/egusphere-2025-6006
Preprint. Discussion started: 18 December 2025


different surface thermal patterns. The following section will focus on specific upwelling events that occurred in autumn and spring.

## 5. Specific Upwelling events during spring and autumn

We selected events with distinct SSTa characteristics and studied 6 cases in total (3 during each season). Across the analyzed cases, positive SSSa were simulated, accompanied by varying surface thermal and heat flux patterns. Additionally, positive vertical velocity anomalies were consistently found near the coast in all the analyzed cases, indicating upwelling (Figure 11). When analyzing the specific events, we observed that the closer the event occurred to the summer, the more it resembled the typical summer upwelling pattern (with saltier and colder water reaching the surface), (Figs. 8-12).

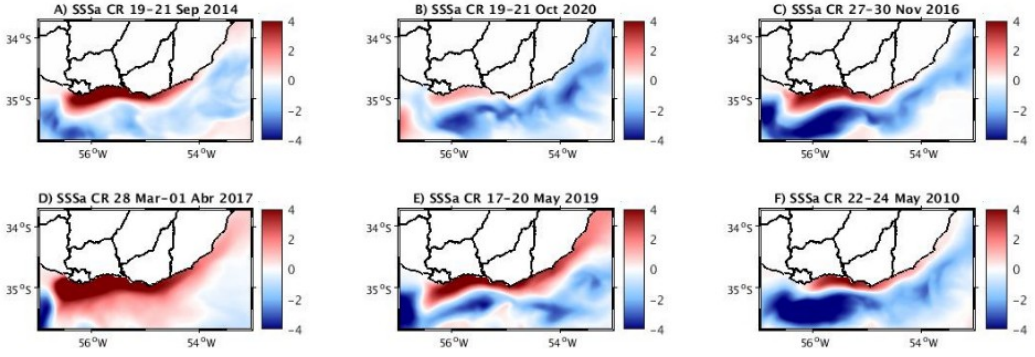


Figure 8: Average simulated Sea Surface Salinity anomalies (SSSa) distribution during selected upwelling events

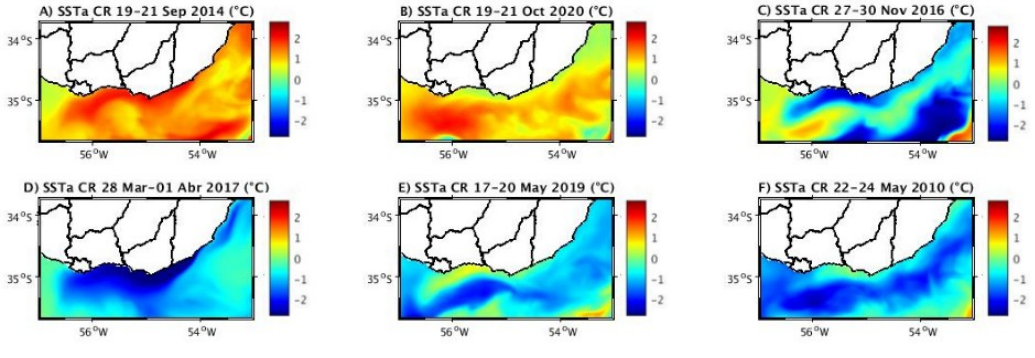


Figure 9: Average simulated Sea Surface Temperature anomalies distribution during selected upwelling events.

https://doi.org/10.5194/egusphere-2025-6006
Preprint. Discussion started: 18 December 2025


During spring, one event for each month was analyzed: September (19 - 21 September, 2014), October (19 - 21 October, 2020), and November (27 - 30 November, 2016). The September event exhibited positive SSSa and SSTa near the coast, together with also positive SSTa offshore but less intense. In concordance with the surface pattern the vertical section shows anomalously warm water not vertically stratified close to the coast (indicating upwelling) and warmer subsurface water reaching the surface during the upwelling (Figs. 9A and 10A). There is also simulated heat lost to the atmosphere, maximum in the upwelling region, also concordant with warm water upwelling (Figure 12 A). During the October event, close to zero SSTa were observed in the coastal region together with positive SSTa offshore (Figs. 9B and 10B). Contrary to the September event, during October in the upwelled water region there is no heat loss to the atmosphere (Figure 12B). Finally, the November event displayed a similar pattern to the summer upwelling events described in detail by de Mello et al. (2022a), characterized by saltier and colder water reaching the surface and a gain of heat from the atmosphere buffering the cold water upwelling (Figs. 9C, 10C and 12C).

During autumn, two events were selected in May (17-20 May 2019 and 22-24 May 2010), along with another event occurring between March and April (28 March - 1 April 2017). The March-April event exhibited a similar pattern to the November upwelling event, resembling summer upwellings (Figs. 9F, 10F and 12F). Unlike the spring events (but consistent with the composites of upwelling for each season), the selected May cases showed close to zero and positive SSTa in the upwelling region together with negative SSTa offshore (Figure 9 E and F). In concordance with the surface patterns, during both events the vertical sections show slightly anomalously warm water not vertically stratified close to the coast (indicating upwelling) (Figure 10 E and F). Finally, the heat flux simulated resulted concordant with warmer water reaching the surface during autumn, with a lost of heat in the upwelling region; and a gain of heat from the atmosphere to the anomalously cold water offshore, where the negative SSTa simulated could possibly be related to advection processes (Figure 12 E and F).

https://doi.org/10.5194/egusphere-2025-6006
Preprint. Discussion started: 18 December 2025


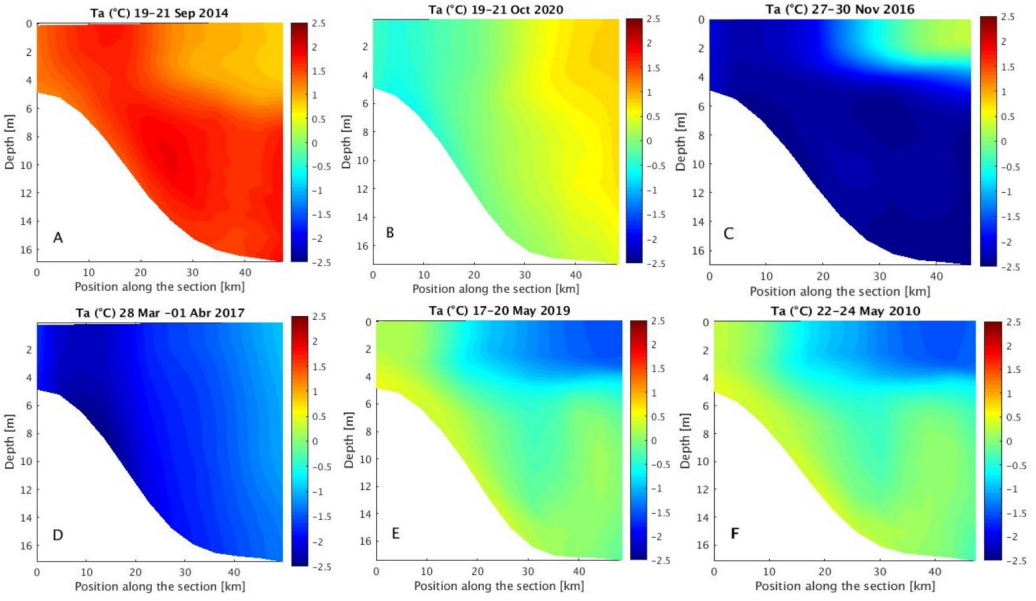


300 Figure 10: Vertical temperature anomalies (Ta) profiles for spring (A-C) and autumn upwelling events (D-F).

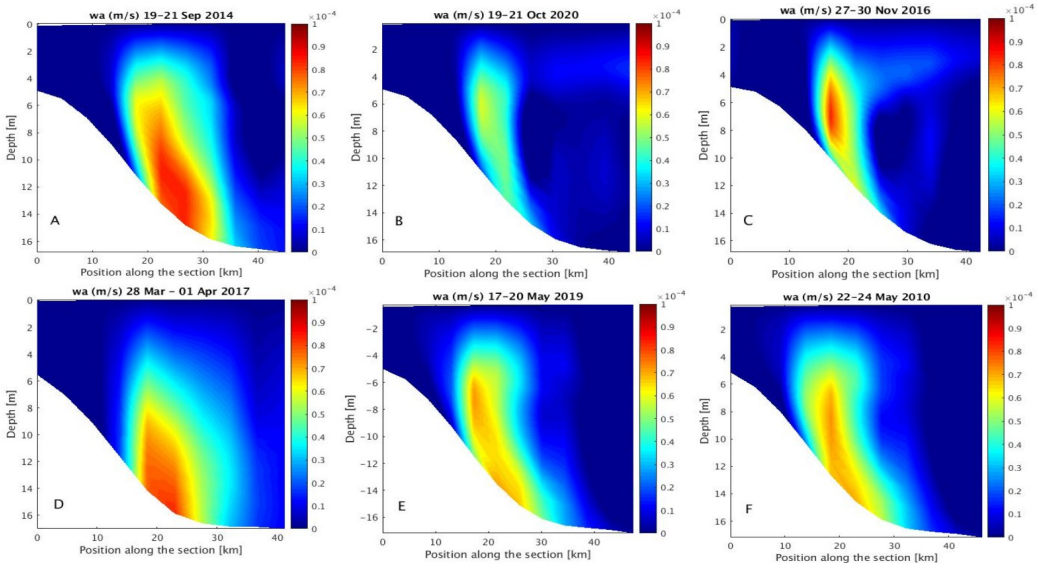


Figure 11: Vertical velocity anomalies (wa) profiles for spring upwelling (A-C) and autumn upwelling events (D-F).

305

https://doi.org/10.5194/egusphere-2025-6006
Preprint. Discussion started: 18 December 2025


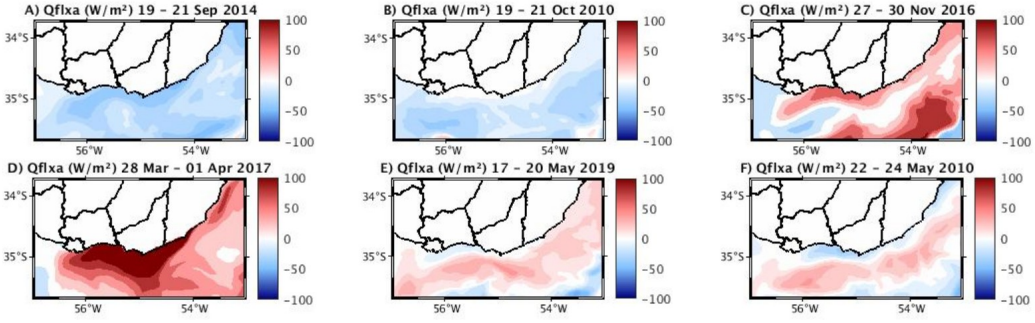


Figure 12: Simulated net heat flux anomalies distribution during selected upwelling events (positive values represents a gain of heat into the ocean)

To conclude, our analysis focused on the 17-20 May 2019 event, as it is the only event with in situ data available for comparison (Trinchin et al., 2024). Both measured and simulated data showed an increase in salinity and temperature during the event. Specifically, in situ salinity increased from around 8 before the event to over 18 during the upwelling, then dropped back to close to 8. Similarly, in situ temperature rose from 16.5°C before the event to 18°C during the upwelling, before falling back to around 16°C (Figure 13A). The model is able to capture the behavior of the two variables both in timing and amplitude, giving credibility to the results presented above. This underscores the value of in situ measurements for detecting upwellings and for validating the model's performance in simulating real processes. Furthermore, the vertical profiles of simulated variables at the Isla de Flores location revealed a stable salinity stratification and an inverse temperature profile prior to the event, transitioning to a mixed water column during the event, characterized by warmer surface temperatures and higher surface salinity compared to earlier dates (Figure 13B-E).

https://doi.org/10.5194/egusphere-2025-6006
Preprint. Discussion started: 18 December 2025


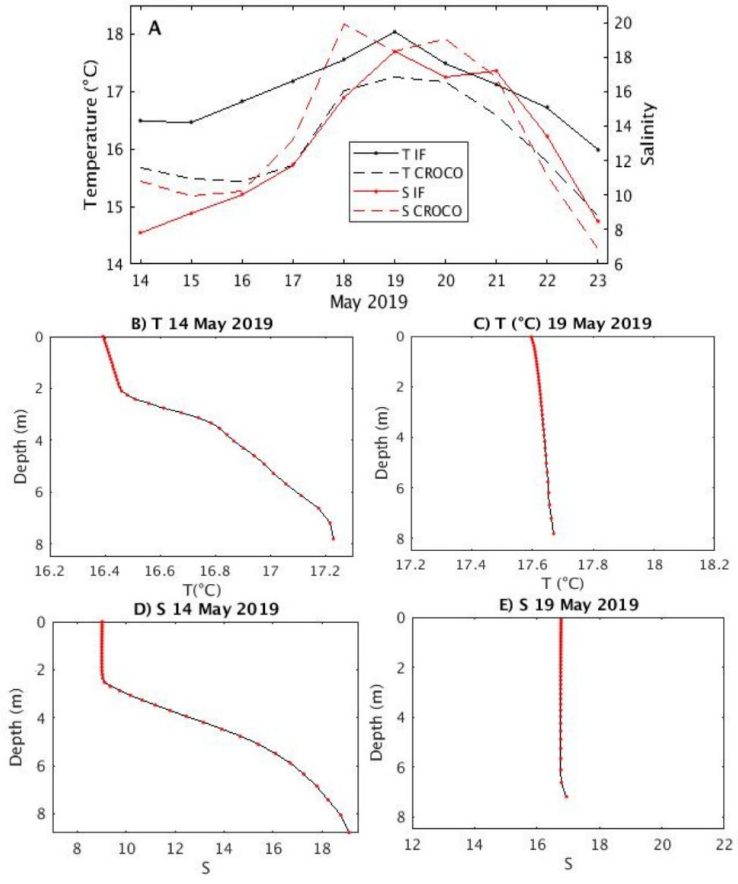


Figure 13: A- In situ (T IF and S IF) and simulated (T CROCO and S CROCO) temperature and salinity at Isla de Flores Location during the period 14-23 May 2019. Simulated vertical profiles of salinity and temperature for 14 and 19 May 2019 at Isla de Flores location (B-E).

## 6. Summary and conclusions

We implemented and validated the CROCO ocean model in an interannual configuration similar to that used by de Mello et al. (2023) to study upwelling processes year-round. The model successfully represented the average and variability conditions throughout the year, accurately capturing salinity and temperature patterns consistent with observational data during both upwelling and not upwelling dates.

Seasonal vertical profiles of temperature and salinity were described for the first time for a coastal location in Uruguay from numerical simulations. These profiles reveal a salinity stratification throughout the year, along with variations in thermal stratification. Thermal stratification was found

https://doi.org/10.5194/egusphere-2025-6006
Preprint. Discussion started: 18 December 2025


during the summer season. In contrast, during both intermediate seasons, there is on average little to no stratification, while in winter the model simulates an inverse thermal profile, with warmer waters near the bottom. These water column characteristics were considered responsible for the differing thermal patterns found during spring and autumn upwelling events.

Upwelling events along the Uruguayan coast were studied throughout the year by analyzing the relationship between zonal wind and sea surface salinity anomalies. Under this approximation upwellings were detected for all seasons, except winter.

As evidenced in previous studies for the summer (de Mello et al., 2022a) or using idealized setups (Meccia et al., 2013), maximum salinity anomalies located in the estuarine coastal region (between Montevideo and Punta del Este) were evidenced during intense upwelling dates irrespective of the season. This is particularly important given the recognized role salinity has in structuring the biological communities in the RdP estuary (Jaureguizar et al., 2004; Giménez et al., 2010; Martínez and Ortega, 2015; Jaureguizar et al., 2016).

As expected, summer upwelling events were characterized not only by positive SSSa but by negative SSTa as well, indicating that both SSTa and SSSa would be reliable indicators for identifying upwelling during this season. In contrast, during spring and autumn, SSSa resulted in a better proxy. In this regard, upwellings were clearly marked by increments in SSSa (which was also evidenced in the in-situ data), but the SSTa pattern in the upwelling region was variable due to different thermal vertical profiles during these seasons. Detailed analysis of specific events was necessary to explain the simulated SSTa distributions.

From the analysis of particular cases, different types of upwelling events could be distinguished based on the thermal characteristics of the upwelled waters: Warm water upwelling events, where anomalously warm deep water is brought to the surface during the upwelling (with varying anomaly intensity). Those are typical from the colder months of spring and autumn and characterized also by a heat loss from the surface water to the atmosphere in the upwelling region. Cold water upwelling events (similar to those occurring in summer) where colder deep water is brought to the surface. Those are typical from the warm season and are characterized also by a heat influx from the atmosphere to the surface water in the upwelling region. And lastly, transitional upwelling events not distinguishable from SSTa, that occur when there is not a marked thermal stratification. Those are also characterized by almost no heat flux anomalies in the upwelling region near the coast.

Given the limited oceanographic data with extensive spatial and temporal coverage of the water column properties, model simulations as the ones of the present study provide a valuable dataset for

https://doi.org/10.5194/egusphere-2025-6006
Preprint. Discussion started: 18 December 2025


describing processes along the Uruguayan coast throughout the year. However, it is crucial to emphasize the importance of having in situ oceanographic data with broad spatial temporal coverage to validate and correct biases in the simulations. This would make the models more realistic, improve the representation of oceanographic processes, and enable more accurate explanations.

Finally, this study represents a first identification of wind induced upwelling events year round in the Uruguayan coast. Considering the amount and diversity of human activities currently taking place in the Uruguayan coastal and adjacent marine region (e.g. hydrocarbon exploration, transport, tourism, and fishing), the consequences of upwelling events occurring outside of summer in the resuspension of sediments, productivity, frontal regions and transport mechanisms are important issues that future studies should include in order to better assess the upwelling socio-ecological importance.

**Author contributions**

C. de Mello designed the study, performed the numerical simulations, carried out the analyses, and wrote the manuscript. M. Barreiro supervised the work, contributed to the interpretation of the results, and participated in the revision and editing of the manuscript. M. Renom supervised the study. All authors approved the final version of the manuscript.

**Declaration of competing interest**

The authors declare that they have no known competing financial interests or personal relationships that could have appeared to influence the work reported in this paper.

**References**

Acha, E. M., Mianzan, H., Guerrero, R., Carreto, J., Giberto, D., Montoya, N., & Carignan, M. (2008). An overview of physical and ecological processes in the Rio de la Plata Estuary. Continental shelf research, 28(13), 1579-1588.

Amante, C., & Eakins, B. W. (2008). ETOPO1 1 Arc-Minute Global Relief Model: Procedures, Data Sources and Analysis: Washington. *DC (DOC/NOAA/NESDIS/NGDC)*.

BaRDO INIDEP database. CTD data obtained from: https://catalogo.inidep.edu.ar/geonetwork/srv/spa/catalog.search#/home

https://doi.org/10.5194/egusphere-2025-6006
Preprint. Discussion started: 18 December 2025


Borús, J. (2022). Evaluación de caudales diarios descargados por los grandes ríos del sistema del Plata al Río de la Plata. Dirección de Sistemas de Información y Alerta Hidrológico Instituto Nacional del Agua, Ezeiza, Argentina.

Baldoni, A. G., Molinari, G., Reta, R., & Guerrero, R. A. (2015). *Atlas de temperatura y salinidad de la plataforma continental del Atlántico Sudoccidental: períodos cálido y frío*. Instituto Nacional de Investigación y Desarrollo Pesquero (INIDEP).

Brum, A. (2024). Variabilidad de la salinidad en la zona media del Río de la Plata y su impacto sobre la productividad primaria en la costa Atlántica Uruguaya. Tesina para la obtención del grado: Licenciada en Cs Biológicas. Facultad de Ciencias, UdelaR, 43p.

Burone, L., Ortega, L., Franco-Fraguas, P., Mahiques, M., García-Rodriguez, F., Venturini, N., ... & Salaroli, A. (2013). A multiproxy study between the Río de la Plata and the adjacent South-western Atlantic inner shelf to assess the sediment footprint of river vs. marineinfluence. *Continental shelf research*, *55*, 141-154.

Debreu, L., Marchesiello, P., Penven, P., & Cambon, G. (2012). Two-way nesting in split-explicit ocean models: algorithms, implementation and validation. *Ocean Modelling*, *49*, 1-21.

de Mello, C., Barreiro, M., Ortega, L., Trinchin, R., & Manta, G. (2022a). Coastal upwelling along the Uruguayan coast: Structure, variability and drivers. Journal of Marine Systems, 230, 103735.

de Mello, C., Barreiro, M., Marin, Y., Ortega, L., Trinchin, R., & Manta, G. (2022b). Relación entre frentes de convergencia y localización de la flota pesquera durante la ocurrencia de surgencia costera en Uruguay. *Innotec*, (24 jul-dic), e624-e624.

de Mello, C., Barreiro, M., Hernandez-Garcia, E., Trinchin, R., & Manta, G. (2023). A Lagrangian study of summer upwelling along the Uruguayan coast. *Continental Shelf Research*, *258*, 104987.

Guerrero, R. A. & Piola, A. R. (1997). Masas de agua en la plataforma continental. http://hdl.handle.net/1834/1703. Accessed 19 August 2024

Guerrero, R.A., Acha, E.M., Framin, M.B. & Lasta, C.A. (1997). Physical oceanography of the Río de la Plata Estuary, Argentina. Cont. Shelf Res. 17 (7), 727–742.

Guerrero, R.A., Piola, A.R., Molinari, G.N., Osiroff, A.P & Jáuregui, S.I. (2010). Climatología de temperatura y salinidad en el Río de la Plata y su Frente Marítimo. Argentina-Uruguay. Instituto Nacional de Investigación y Desarrollo Pesquero, Contribución no 1555. Mar del Plata, ISBN. 978-987-1443-03-1.

https://doi.org/10.5194/egusphere-2025-6006
Preprint. Discussion started: 18 December 2025


Kanamitsu, M., Ebisuzaki, W., Woollen, J., Yang, S. K., Hnilo, J. J., Fiorino, M., & Potter, G. L. (2002). Ncep–doe amip-ii reanalysis (r-2). *Bulletin of the American Meteorological Society*, *83*(11), 1631-1644.

Largier, J. L. (2020). Upwelling bays: How coastal upwelling controls circulation, habitat, and productivity in bays. *Annual review of marine science*, *12*(1), 415-447. DOI: 10.1146/annurev-marine-010419-011020.

Lellouche, J. M., Le Galloudec, O., Greiner, E., Garric, G., Regnier, C., Drevillon, M., & Le Traon, P. Y. (2018). The Copernicus Marine Environment Monitoring Service global ocean 1/12? physical reanalysis GLORYS12V1: description and quality assessmen. In *EGU General Assembly Conference Abstracts* (Vol. 20, p. 19806).

Martínez, A., Ortega, L. (2015). Delimitation of domains in the external Río de la Plata estuary, involving phytoplanktonic and hydrographic variables. Braz. J. Oceanogr. 63 (3), 217–227.

Meccia, V.L., Simionato, C.G., Guerrero, R.A. (2013). The Rio de la Plata Estuary response to wind variability in synoptic timescale: salinity fields and salt wedge structure. J. Coast. Res. 29 (1), 61–77.

Möller Jr., O.O., Piola, A.R., Freitas, A.C., et al. (2008). The effects of river discharge and seasonal winds on the shelf off southeastern South America. Cont. Shelf Res. 28 (13), 1607–1624.

Nagy, G. J., Gómez-Erache, M., López, C. H., & Perdomo, A. C. (2002). Distribution patterns of nutrients and symptoms of eutrophication in the Rio de la Plata River Estuary System. In *Nutrients and eutrophication in estuaries and coastal waters* (pp. 125-139). Springer, Dordrecht.

Ortega, L., & Martínez, A. (2007). Multiannual and seasonal variability of water masses and fronts over the Uruguayan shelf. Journal of Coastal Research, 23(3), 618-629.

Piola, A.R., Campos, E.J.D., Möller Jr., O.O., et al. (2000). Subtropical shelf front off eastern South America. J. Geophys. Res. 105 (C3), 6565–6578.

Piola, A. R., Matano, R. P., Palma, E. D., Möller Jr, O. O., & Campos, E. J. (2005). The influence of the Plata River discharge on the western South Atlantic shelf. *Geophysical Research Letters*, *32*(1).

Piola, A. R., M¨oller Jr, O. O., Guerrero, R. A., and Campos, E. J. D. (2008). Variability of the Subtropical Shelf front off eastern SouthAmerica: winter 2003 and summer 2004, Cont. Shelf Res., 28, 1639–1648, doi:10.1016/j.csr.2008.03.013.

https://doi.org/10.5194/egusphere-2025-6006
Preprint. Discussion started: 18 December 2025


Pimenta, F., Garvine, R. W., & Münchow, A. (2008). Observations of coastal upwelling off Uruguay downshelf of the Plata estuary, South America. *Journal of Marine Research*, *66*(6), 835-872.

Pitcher, G. C., Figueiras, F. G., Hickey, B. M., & Moita, M. T. (2010). The physical oceanography of upwelling systems and the development of harmful algal blooms. *Progress in Oceanography*, *85*(1-2), 5-32.

Rabellino, J. (2016). Análisis del rol del frente subtropical de plataforma sobre huevos y larvas de engraulis anchoita utilizándo un enfoque bio-físico. Pedeciba Geociensce Master Thesis. Tesis, PEDECIBA-GEOCIENCIAS, UdelaR, 129 p

Shchepetkin, A. F., & McWilliams, J. C. (2005). The regional oceanic modeling system (ROMS): a split-explicit, free-surface, topography-following-coordinate oceanic model. Ocean modelling, 9(4), 347-404.

Simionato, C. G., Vera, C. S., & Siegismund, F. (2005). Surface wind variability on seasonal and interannual scales over Río de la Plata area. *Journal of Coastal Research*, *21*(4), 770-783.

Simionato, C.G., Tejedor, M.L.C., Campetella, C., Guerrero, R., Moreira, D. (2010). Patterns of sea surface temperature variability on seasonal to sub-annual scales at and offshore the Río de la Plata estuary. Cont. Shelf Res. 30 (19), 1983–1997.

Steger, J.M., Schwing, F.B., Collins, C.A., Rosenfeld, L.K., Garfield, N., Gezgin, E. (2000). The circulation and water masses in the Gulf of the Farallones. Deep Sea Research Part II. Topical Stud. Oceanogr. 47 (5–6), 907–946.

Trinchin, R., Ortega, L.; Barreiro, M. (2019). Spatiotemporal characterization of summer coastal upwelling events in Uruguay, South America. Regional Studies in Marine Science, 31, 100787.

Trinchin, R., Manta, G., Santana, R., Rubio, L., Horta, S., Passadore, C., Barreiro, M. (2021). Hacia un monitoreo continuo de variables oceanográficas en el Parque Nacional Isla de Flores, Uruguay. Innotec, p. 21.

Trinchin, R., Manta, G., Horta, S., Barreiro, M., Santana, R., Rubio, L. (2024). "Temperatura y Salinidad en Isla de Flores con resolución horaria", ttps://doi.org/10.60895/redata/X3FUPX, Repositorio de datos abiertos de investigación de Uruguay, V1, UNF:6:SqgKYqU2zQD8f6hy1LetsQ== [fileUNF]

Wallace, J. M., Smith, C., & Bretherton, C. S. (1992). Singular value decomposition of wintertime

https://doi.org/10.5194/egusphere-2025-6006
Preprint. Discussion started: 18 December 2025


490 sea surface temperature and 500-mb height anomalies. Journal of climate, 5(6), 561-576.